

Supplementary Information for

# **Local Structures of Garnet-type Solid Electrolyte Densified by Spark Plasma Sintering**

Hirotooshi Yamada<sup>\*</sup>, Tomoko Ito, Rajendra Hongahally Basappa

Graduate School of Engineering, Nagasaki University

1-14, Bunkyo-machi, Nagasaki, 852-8521 Japan

\*h-yama@nagasaki-u.ac.jp

### S1. Rietveld refinement of LLZT pellets

Figure S1(a) shows XRD profiles of a LLZT pellet densified by SPS, fitted by a structure model consisting of cubic and tetragonal LLZT (Table S1).

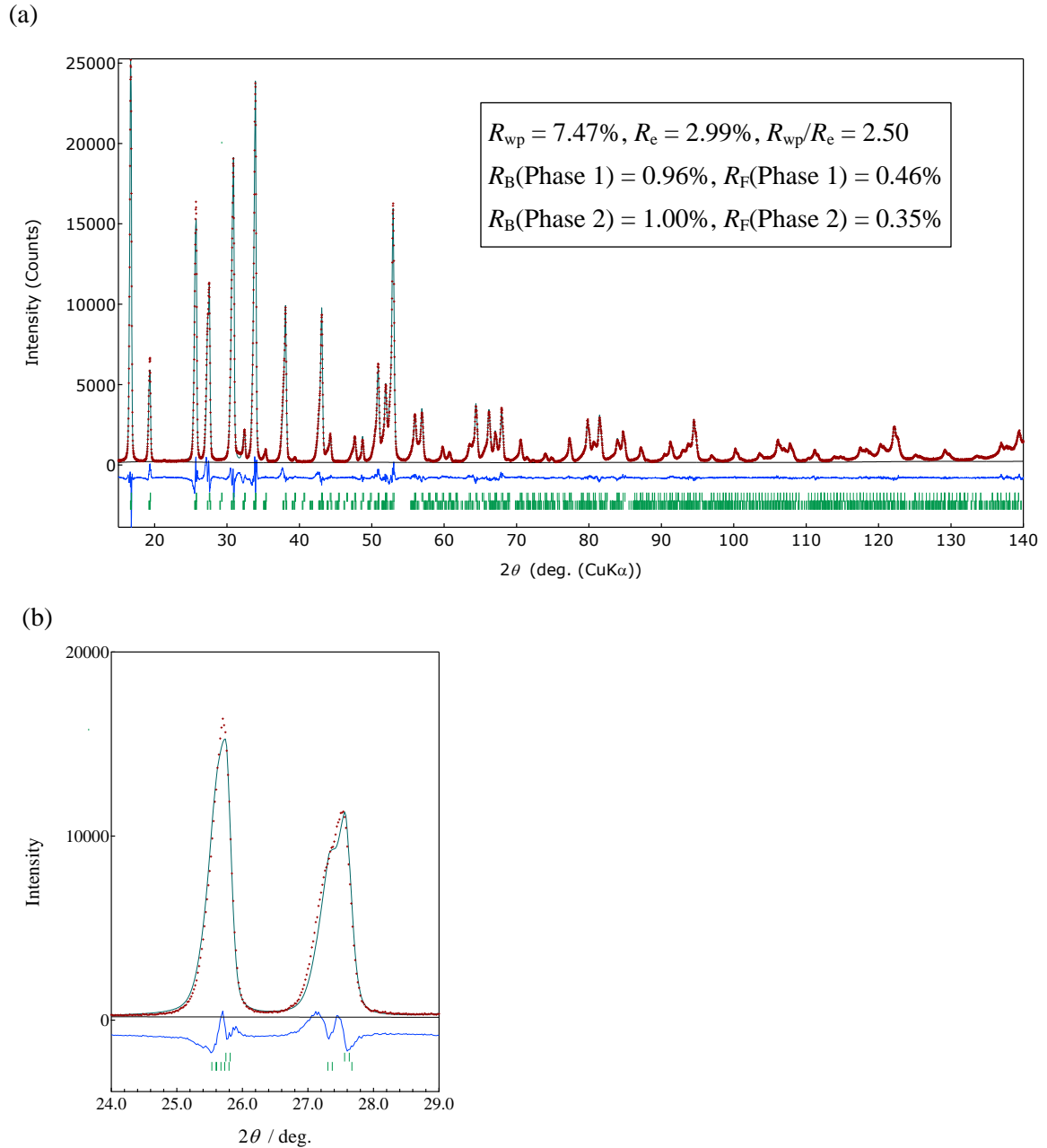


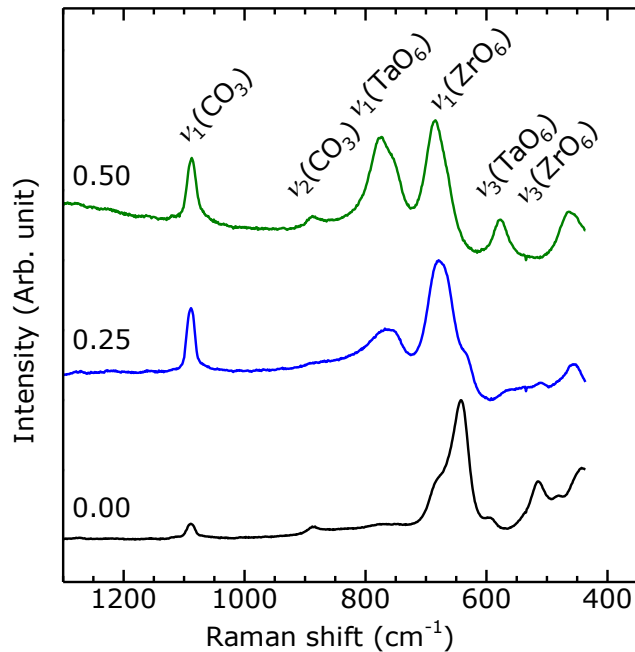
**Figure S1.** (a) XRD profiles of a LLZT pellet densified by SPS and fitting profiles using a model consisting of cubic and tetragonal LLZT. Reliability indices are shown in the figure. (b) Enlarged profiles of (a).

**Table S1.** Structural parameters of LLZT phases contained in a LLZT pellet sintered by SPS.

	Phase 1 (cubic LLZT)	Phase 2 (tetragonal LLZT)
Space group	$Ia-3d$ (No. 230)	$I4_1/acd$ (No. 142)
Lattice parameters	$a = 12.9354(3)$	$a = 13.055$ (1) $c = 12.885$ (2)
Weight ratio	65.0%	35.0%

## S2. Formation of $\text{Li}_2\text{CO}_3$

Formation of  $\text{Li}_2\text{CO}_3$  was studied by Raman and transmission electron microscopy (TEM, JEOL JEM-2010 UHR). Raman spectra was recorded on a RMP-210 (JASCO Corp.) with 532 nm laser (100 mW). Figure S2 shows Raman spectra of  $\text{Li}_{7-x}\text{La}_3\text{Zr}_{2-x}\text{Ta}_x\text{O}_{12}$  powder with different amount of doped Ta ( $x = 0, 0.25, 0.5$ ).  $\text{CO}_3^{2-}$  was clearly detected around  $1100\text{ cm}^{-1}$ . A TEM image of LLZT powder exhibits an amorphous layer covering the surface of a particle with a thickness of 5-100 nm. In Raman spectra (Figure S2), apparently, carbonate increases with increasing  $x$  in  $\text{Li}_{7-x}\text{La}_3\text{Zr}_{2-x}\text{Ta}_x\text{O}_{12}$ . However, it should be noted that the spectra are normalized by  $\nu_1(\text{ZrO}_6)$  that also decreases with increasing  $x$ .

**Figure S2.** Raman spectra of garnet-type solid electrolyte  $\text{Li}_{7-x}\text{La}_3\text{Zr}_{2-x}\text{Ta}_x\text{O}_{12}$  powder. Intensity is normalized by  $\nu_1(\text{ZrO}_6)$ .

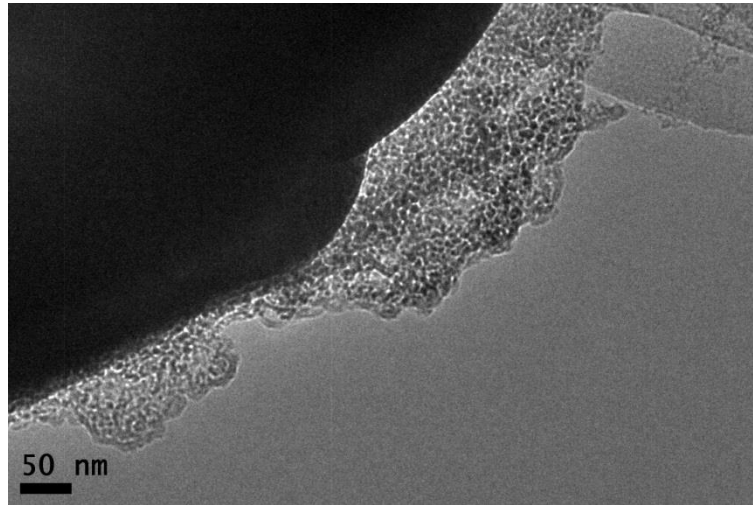


**Figure S3.** TEM image of LLZT powder.

### **S3. Deformation of LLZT particles on SPS**

Figure S4(a) and S4(b) show SEM images of LLZT powder and fractured cross-section of a LLZT pellet. Note that pressure was applied along horizontal direction of Figure S4(b) on SPS.

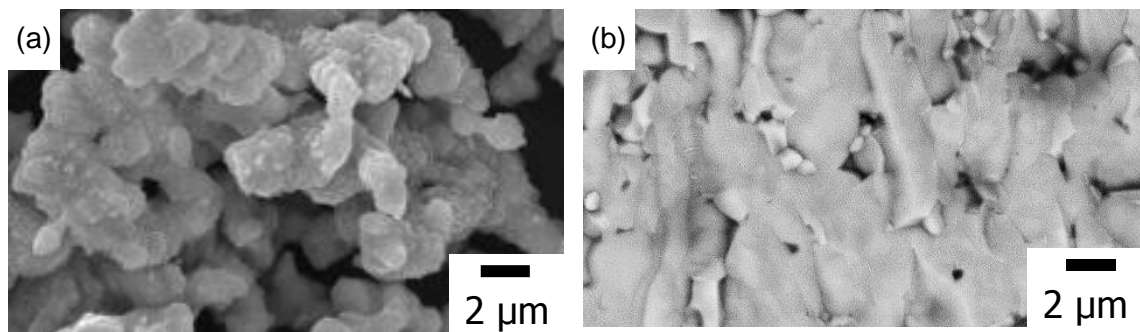


**Figure S4.** SEM images of LLZT (a) powder and (b) pellet.

#### S4. Attenuation length of X-ray in LLZT

Figure S5 shows attenuation length of X-ray ( $\lambda = 0.154$  nm) as a function of grazing angle, which was calculated on the Web (X-Ray Interactions With Matter, [http://henke.lbl.gov/optical\\_constants/](http://henke.lbl.gov/optical_constants/)). In the calculation, density of LLZT is assumed to be  $5.36 \text{ g cm}^{-3}$  (relative density: 100%).

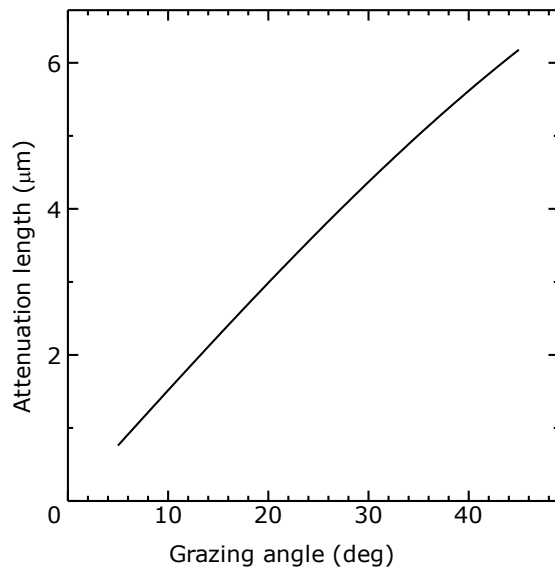


**Figure S5.** Attenuation length of X-ray ( $\lambda = 0.154$  nm).

#### S4. X-ray photoelectron spectroscopy (XPS)

XPS was conducted on an AXIS-ULTRA DLD (Kratos Analytical Ltd.) with a monochromated AlK $\alpha$  (photon energy: 1.4867 keV, 15 kV, 10 mA). Spectra were recorded for C1s, Li1s, La3d, Zr3p, Ta4d and O1s with a pass-energy of 40 eV. Spectra were taken on a point where dark stain was observed, i.e. near the cathode of SPS on fractured cross-section of a LLZT pellet as shown in Figure S5. To avoid the reaction of LLZT with H<sub>2</sub>O and CO<sub>2</sub> in the atmosphere, the pellet was taken out of dies and broken into pieces in an Ar-filled glovebox, and the specimen was transferred to XPS chamber without exposure to air. The spot size of X-ray was ca. 300  $\times$  700  $\mu$ m and the center of the spot is indicated by a red cross in Figure S5. Contaminant carbon (285.0 eV) on the surface of specimen was used for calibration of binding energy.

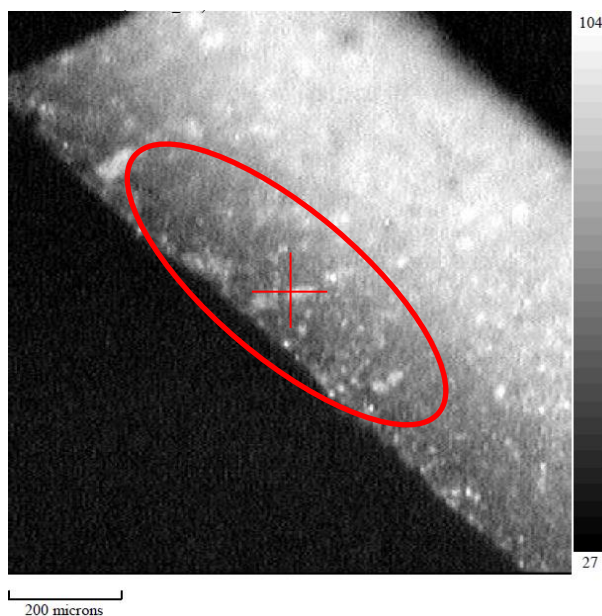


**Figure S5.** The optical image of the specimen for XPS. A red cross and an ellipsoid indicate the irradiation area of X-ray.

Figure S6 shows XPS of La 3d<sub>5/2</sub>, Ta 4d and Zr 3p. For La 3d<sub>5/2</sub>, three peaks were confirmed at 834.1, 836.1 and 838.6 eV. The peak at 834.1 eV is attributed to La<sup>3+</sup> as in La<sub>2</sub>O<sub>3</sub>. The split of La 3d spectrum is explained by the charge transfer effect from the surrounding oxygens to the 4f orbitals of La<sup>3+</sup> [S1, S2]. Ta 4d and Zr 3p spectra indicate both elements are in a single oxidation state. Ta 4d<sub>5/2</sub> at 225.4 eV and Zr 3p<sub>3/2</sub> at 332.1 eV are assigned to Ta<sup>5+</sup> and Zr<sup>4+</sup>, respectively. Therefore, it is confirmed that all the transition metal ions are not reduced on SPS.

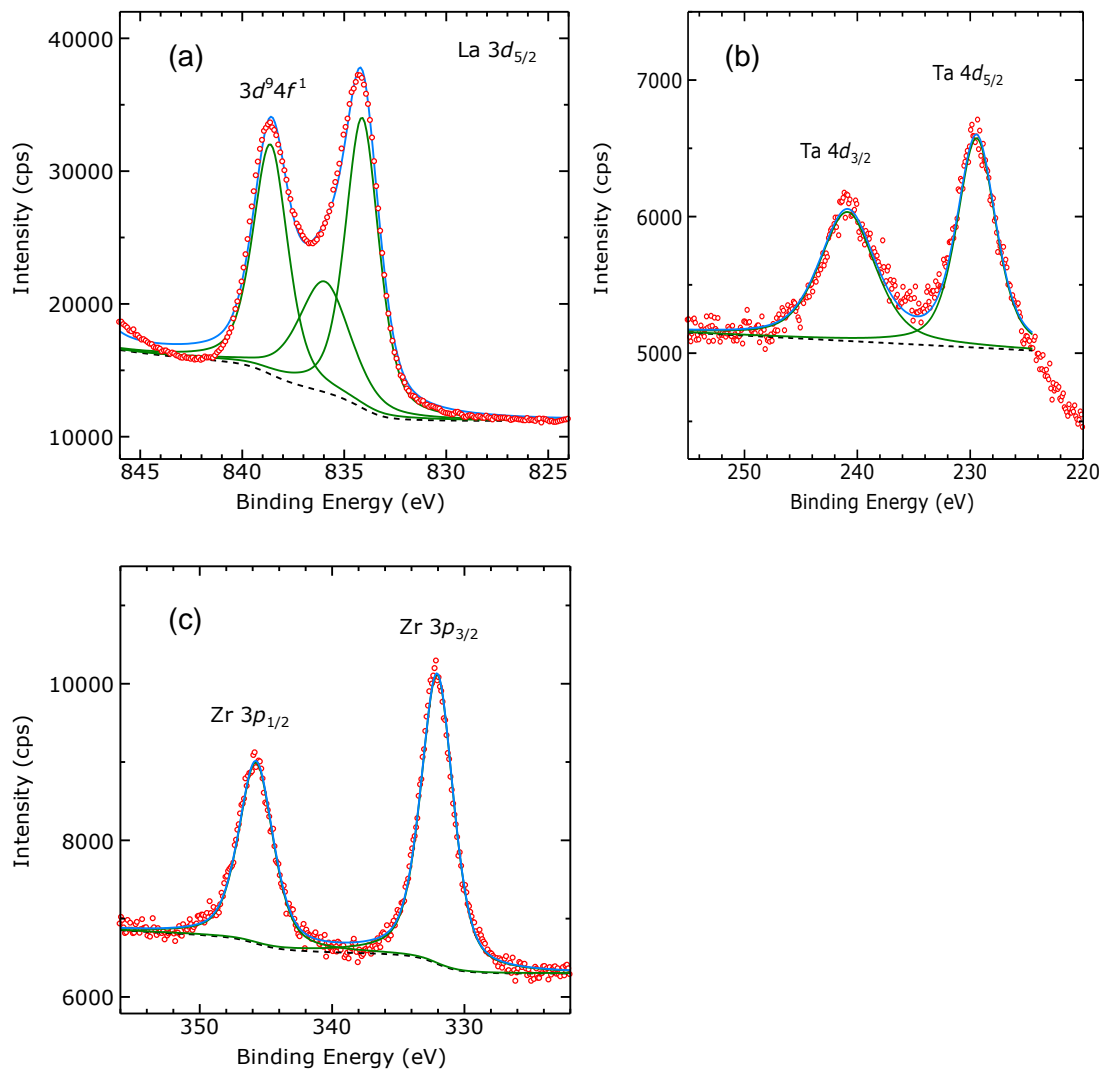


**Figure S6.** XPS spectra of cathode side of fractured cross-section of a LLZT pellet. (a) La  $3d_{5/2}$ , (b) Ta  $4d$  and (c) Zr  $3p$ .

### S5. Electromigration on cathode

In order to demonstrate the electromigration on SPS, a LLZT pellet was prepared by SPS using Au foil between LLZT powder and graphite dies as explained in the main text. Figure S7(a) exhibits a reflection electron image of cross-section of the pellet. There are several bright spots in the image as in Figure 6. To confirm the origin of these spots, EDS mapping images were taken for La, Ta, O, Au and C (Figure S7(b)~(f)). Intense Au signal was clearly confirmed at bright spots (Note that background signal of Au is due to the Au thin layer (ca. 20 nm in thickness) was deposited on the specimen to avoid being charged).

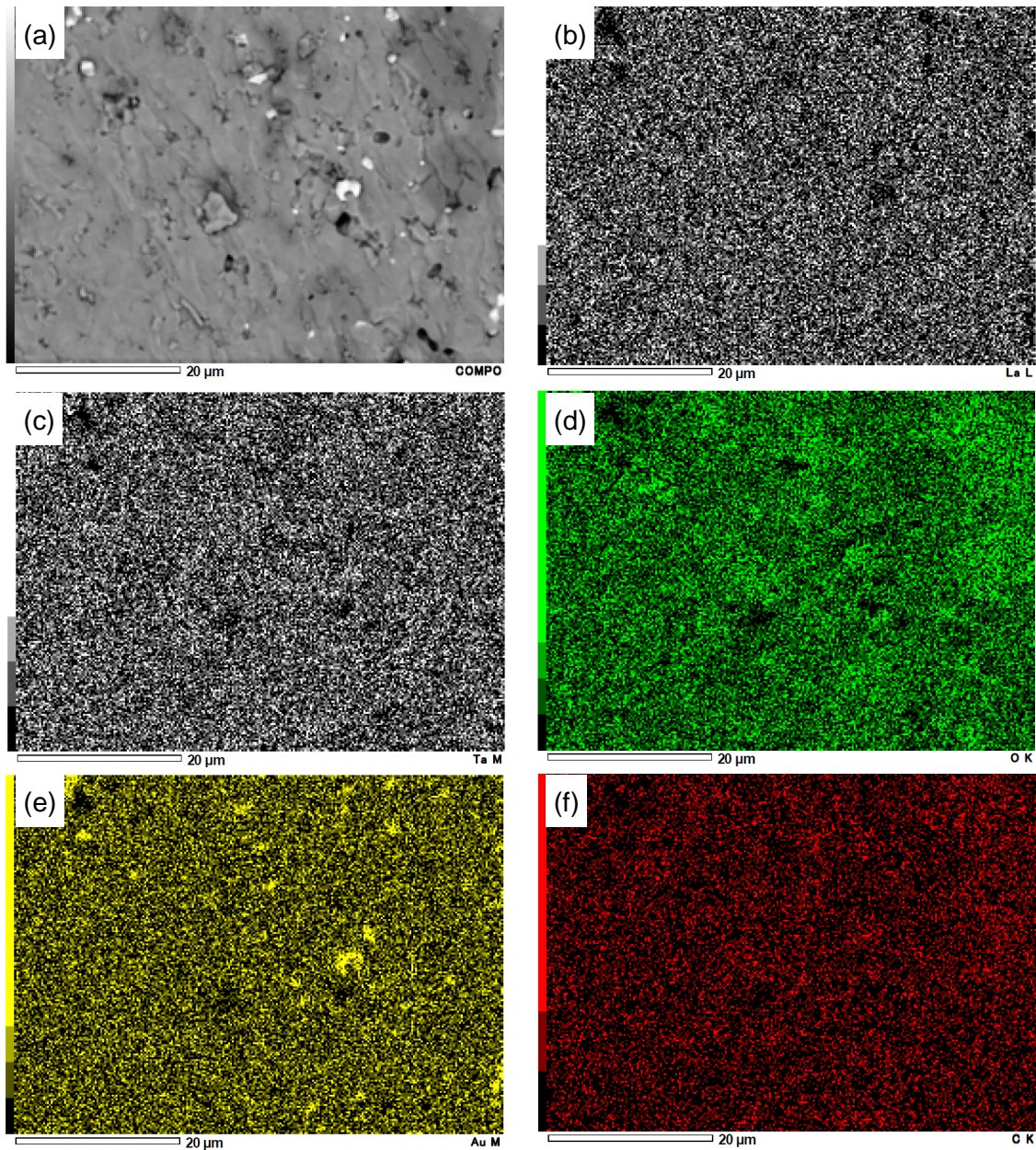


**Figure S7.** Fractured cross-sectional images of a LLZT pellet. (a) A reflection electron image and (b~f) EDS mapping images for the same area.



## S6. Electrochemical analysis of LLZT pellets densified by SPS

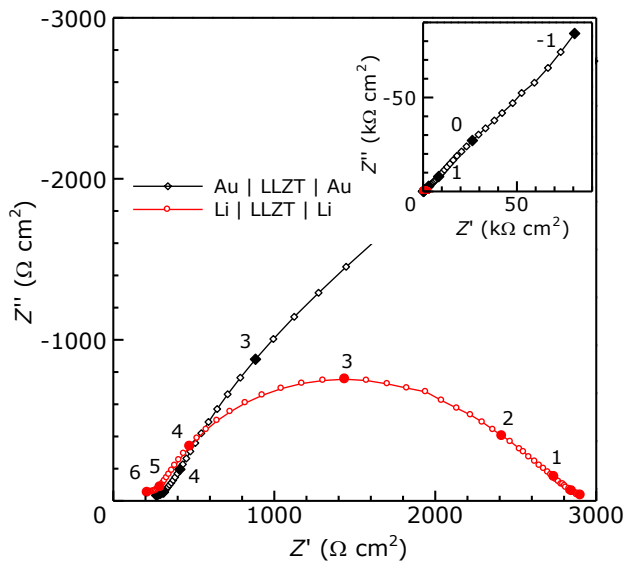


**Figure S8** Nyquist plots of symmetric cells with Au electrodes and Li electrodes. Numbers on the plots denote common logarithms of frequencies.

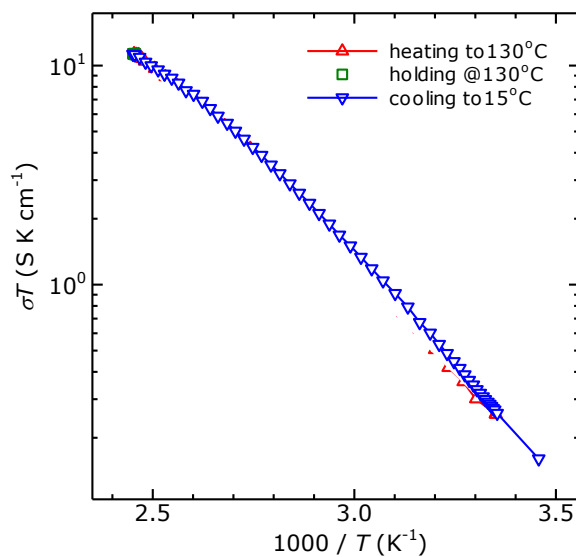


**Figure S9.** Temperature dependence of ionic conductivity recorded with scanning temperature at a very slow ramp rate of  $0.25^\circ\text{C}/\text{min}$ .

**Table S1.** Comparison of LLZT prepared by various sintering techniques.

Ta composition <sup>a</sup>	Sintering technique	Pressure (MPa)	Temperature (°C)	Duration (min)	Relative density (%)	Total conductivity @298 K (S cm <sup>-1</sup> )	Activation energy (eV)	Reference
0.5	SPS	37.5	1000	10	95.5	6.90×10 <sup>-4</sup>	0.42	this work
0.5	SPS	50	1000	10		1.35×10 <sup>-3</sup>	0.41	[26]
0.5	conventional		1200	1200		5.22×10 <sup>-4</sup>	0.32	[26]
0.5	conventional		1100	900	89	6.10×10 <sup>-4</sup>	0.40	[S3]
0.4	hot press	50	1150	120	99	1.18×10 <sup>-3</sup> *	0.4	[24]
0.5	hot press	62	1050	60	97.8	8.16×10 <sup>-4</sup>	0.431	[32]

<sup>a</sup>  $x$  in Li<sub>7-x</sub>La<sub>3</sub>Zr<sub>2-x</sub>Ta<sub>x</sub>O<sub>12</sub>, \* Total conductivity at 303 K

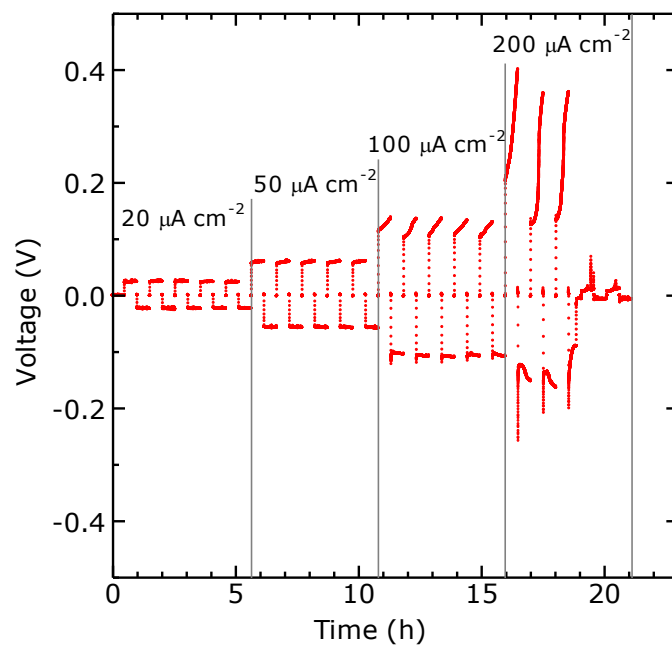


**Figure S10.** Dc polarization curves of a symmetric cell Li | LLZT | Li at 298 K. The thickness of pellets was 1.81 mm.

## References

- [S1] C. Suzuki, J. Kawai, M. Takahashi, A.-M. Vlaicu, H. Adachi, T. Mukoyama, *Chem. Phys.* 253 (2000) 27-40.
- [S2] T. Honma, Y. Benino, T. Fujiwara, T. Komatsu, R. Sato, V. Dimitrov, *J. Appl. Phys.* 91 (2002) 2942-2950.
- [S3] R. Inada, K. Kusakabe, T. Tanaka, S. Kudo, Y. Sakurai, *Solid State Ionics* 262 (2014) 568-572.